



1 **Characterizing the spatial variations and correlations of**
2 **large rainstorms for landslide study**

3

4 **Liang Gao¹, Limin Zhang¹ and Mengqian Lu¹**

5 ¹Department of Civil and Environmental Engineering, The Hong Kong University of Science
6 and Technology, Clear Water Bay, Hong Kong

7 *Correspondence to:* L. M. Zhang (cezhangl@ust.hk)

8

9 **Abstract**

10 Rainfall is the primary trigger of landslides in Hong Kong; hence rainstorm spatial distribution
11 is an important piece of information in landslide hazard analysis. The primary objective of this
12 paper is to quantify spatial correlation characteristics of three landslide-triggering large storms
13 in Hong Kong. The spatial maximum rolling rainfall is represented by a rotated ellipsoid trend
14 surface and a random field of residuals. The maximum rolling 4-h, 12-h, 24-h and 36-h rainfall
15 amounts of these storms are assessed via surface trend fitting, and the spatial correlation of the
16 detrended residuals is determined through studying the scales of fluctuation along eight
17 directions. The principal directions of the surface trend are between 19° and 43°, and the major
18 and minor axis lengths are 83-386 km and 55-79 km, respectively. The scales of fluctuation of
19 the residuals are found between 5 km and 30 km. The spatial distribution parameters for the
20 three large rainstorms are found to be similar to those for four ordinary rainfall events. The
21 proposed rainfall spatial distribution model and parameters help define the impact area, rainfall
22 intensity and local topographic effects for landslide hazard evaluation in the future.



23 **1 Introduction**

24 Severe rainstorms are one of the most dangerous meteorological phenomena which pose risks
25 to human lives and properties. A large rainstorm may cause serious damage to infrastructures
26 and public safety. For instance, a large storm hit Lantau Island, Hong Kong, on 5-7 June 2008
27 and caused about 2,400 natural terrain landslides and 622 flooding spots (CEDD, 2009). In
28 hazards mitigation and engineering design, certain ‘design storms’ must be considered and the
29 engineering system should be sufficiently safe under such design storms (Gao et al., 2015). A
30 design storm is often defined by a hyetograph (time distribution) and an isohyet (spatial
31 distribution). For a particular region where the spatial rainfall variation is significant, a uniform
32 representation of the spatial distribution is not reasonable since a storm has a centre and
33 influences a limited area (AECOM and Lin, 2015). Instead, relevant spatial variation factors of
34 rainfall must be characterized, such as the geometry of spatial form (agglomerate and local
35 gradient) and the spatial correlation.

36 A storm is difficult to model due to its intermittence (i.e. no rainfall at a particular position
37 during a particular short period) and strong spatial and temporal heterogeneity (e.g.,
38 Barancourt et al., 1992; Bacchi and Kottegoda, 1995; Mascaro, 2013). However, the rainfall
39 amount, which is in form of regionalized variables, is spatially correlated over a certain
40 distance (Panthou et al., 2014; de Luca, 2014). A regionalized variable is any variable
41 distributed in space. Random field theory is recognized as a suitable theory for describing
42 regionalized variables (Vanmarcke, 1977) and has been proven effective for the regionalized
43 variables (e.g., Dasaka and Zhang, 2012; Li et al., 2015). The random field theory has also been
44 used in spatial storm analysis (e.g., Rodríguez-Iturbe, 1984; Bouvier, 2003), and adopted to
45 describe storm spatial structures (e.g., Zawadzki, 1973; Lebel et al., 1987; Gyasi-Agyei and
46 Pegram, 2014).

47 Research on spatial rainfall distribution using statistical models has been performed in



48 Hong Kong for different engineering purposes (Leung and Law, 2002; Jiang and Tung, 2014;
49 AECOM and Lin, 2015). Leung and Law (2002) conducted kriging analysis on Hong Kong
50 hourly rainfall data in 1997 and 1998. Rainfall contours were interpolated to qualitatively
51 estimate possible flooding locations. Jiang and Tung (2014) derived rainfall
52 depth-duration-frequency relations at ungauged sites in Hong Kong using an ordinary kriging
53 approach based on annual maximum daily rainfall data. The extreme rainfall estimates are
54 sensitive to assumed statistical parameters and uncertainties of the interpolation method.

55 The storm characteristics such as distribution form and spatial correlation are not
56 sufficiently analysed when studying the hydrological response of a target system such as a
57 slope safety system. In particular, limited attention has been paid to event-based spatial
58 characteristics of large rainstorms in Hong Kong, whose patterns and structures are as useful as
59 the statistical trend based on historic rainfall records, especially when one needs to select large
60 rainstorms for landslide risk assessment. Sufficient information should be provided including
61 both spatial variation and correlation. However, several key questions have not been answered.
62 Can the spatial precipitation distribution of a large storm be represented using a particular
63 spatial form? How does the spatial correlation of rainfall change with the rainstorm magnitude?
64 What are the key factors that influence the spatial structure of rainfall distribution? Such
65 questions motivate the present study on the spatial characteristics of large rainstorms over hilly
66 terrains in Hong Kong.

67 The objective of this paper is to identify the spatial variations and correlation of large
68 rainstorms in Hong Kong. Three large storms that caused the most severe landslide hazards in
69 Hong Kong in the past 20 years are selected for study. These storms were often referred to in
70 Hong Kong as reference storms in preparing engineering measures for landslide hazard
71 mitigation. The results are therefore expected to provide valuable information for landslide
72 hazard analysis and risk management.



73

74 **2 Topography and general rainfall distribution in Hong Kong**

75 Hong Kong is located at the southeast coast of China. The subtropical climate in Hong Kong is
76 characterized by notable dry and wet seasons. About 85% of the annual rainfall is recorded
77 during the wet season from April to September. Storms with high intensity and short duration
78 in Hong Kong are typically associated with southwest monsoon or tropical cyclones. The
79 ground surface elevation on the GIS platform is shown in Fig. 1. The two highest mountain
80 peaks in Hong Kong are Tai Mo Shan (Near rain gauge N14) and Lantau Peak (Near rain gauge
81 N21), with peak elevations of 957 m and 934 m above the sea level, respectively. Both the
82 moisture movements and the topography determine the distribution characteristics (e.g.,
83 agglomerate and local gradient) of rainfall in the spatial domain.

84 AECOM and Lin (2015) studied the orographic factors of rainfall spatial distribution
85 based on historical records. A spatial distribution of orographic intensification factors has been
86 developed based on historical hourly data. The 24-h orographic intensification factors at a
87 resolution of 5 km×5 km are shown in Fig. 2. The factors for the land area are in general larger
88 than those for the sea area. The higher the elevation is, the larger the orographic intensification
89 factor. Two of the highest intensity regions are located at Tai Mo Shan in New Territories and
90 Lantau Peak on Lantau Island. The trend of the factors coincides with the mountain range
91 alignment, i.e., around N45°E.

92 The magnitude of storms can be assessed corresponding to a depth-area relation, and
93 characterized by the probable maximum precipitation (PMP). PMP is frequently used to
94 quantify extreme storm events (WMO, 2009). The scenarios of 4-hour and 24-hour PMP for
95 Hong Kong have been assessed by Hong Kong Observatory and AECOM (Chang and Hui,
96 2001; AECOM and Lin, 2015). AECOM and Lin (2015) updated the 24-h PMP for Hong Kong
97 considering the local orographic intensification. The trend surface is an expected-value



98 surface. The trend surfaces of 24-h PMP with different storm centres have been updated by
99 AECOM and Lin (2015), and the typical trends are shown in Fig. 3. The trend surfaces are
100 derived based on the historical hourly rainfall. According to the 24-h PMP updating study, an
101 elliptical isohyet is recommended as a generalized convergence pattern. For storms centered at
102 Tai Mo Shan, the orientation of 22.5° (N 67.5° E) is found to be the most critical.

103

104 **3 Progression and precipitation data of three large storms**

105 The most traditional way to describe the rainstorm severity is by return period, which is
106 recognized as a combination of intensity and duration. Another measure of the severity of a
107 storm is the consequence of the storm, such as rain-induced landslides or flooding. An index
108 measuring the potential to trigger landslides, named “Landslide Potential Index (LPI)”, is used
109 in Hong Kong (CEDD, 2009). The LPI is based on the historic records of landslide events since
110 1984. For instance, a storm in late July 1994 caused 5 fatalities and its LPI was 10. The value of
111 LPI can be greater than 10 if a storm is more damaging than the July 1994 storm. According to
112 the LPI, the top three largest storms in the past 20 years were the 5-7 June 2008 storm, the
113 17-21 August 2005 storm and the 23 July 1994 storm. Each of these three storms had an LPI
114 around 10 and led to fatalities. Thus, the three storm events are selected as indicative large
115 storms to conduct spatial correlation analysis in this paper.

116 The rainfall data in this study is provided by Geotechnical Engineering Office (GEO) and
117 Hong Kong Observatory (HKO) in Hong Kong. The GEO and HKO rain gauge networks
118 comprise 88 and 46 stations, respectively (Fig. 1). The rain gauges are more concentrated in the
119 northern Hong Kong Island and Kowloon where the population density is high. The raw digital
120 data at 5-minute interval from the high quality network ensures the reliability of this study. The
121 data covers the period from 00:00 on 5 June to 24:00 on 7 June 2008, from 00:00 on 17 August
122 to 24:00 on 21 August 2005, and from 00:00 on 22 July to 24:00 on 24 July 1994. Some of the



123 rain gauges had not been installed in July 1994. The numbers of effective rain gauges for the
124 three events are 105, 112, and 56, respectively. The three storm hyetographs corresponding to
125 the maximum local precipitation depth are shown in Fig. 4. The 17-21 August 2005 storm is
126 more moderate in short durations compared with the 5-7 August 2008 storm and the 22-24 July
127 1994 storm.

128

129 **3.1 The 5-7 June 2008 storm**

130 According to Hong Kong Observatory (HKO), the weather was influenced by an active low
131 pressure trough over the south China coastal area during the first 10 days of June 2008, and was
132 heavily rainy and thundery. Fig. 5 (a) shows contours of the total rainfall amount of the 5-7
133 June 2008 storm. The maximum total rainfall amount was 670 mm. The storm centre was on
134 the southeast of Lantau Island. The magnitudes of the storm characterized by 4-h PMP and
135 24-h PMP (AECOM and Lin, 2015) are shown in Fig. 6. From the depth-area relationships,
136 when the area is in the range of 50 - 1100 km², the maximum rolling 4-h rainfall of the 5-7 June
137 2008 storm has a return period of 1,100 years, corresponding to 60%-67% of the 4-h PMP,
138 while the return period for the 24-h rainfall is 200 years, corresponding to 33%-41% of the
139 24-h PMP. The storm caused 2,400 natural terrain landslides (Li et al., 2009), including many
140 debris flows that affected developed regions, leading to 2 fatalities (CEDD, 2008). The LPI
141 value was recognized as 12. The 4-h maximum rolling rainfall value is calculated as the
142 maximum values of rainfall in 4 consecutive hours on a hyetograph.

143 The maximum rolling rainfall values at different locations may not be in the same period
144 though most of them tend to be in the same period. Hazard consequences are more related to
145 the maximum rolling rainfall values other than instantaneous one (Dai and Lee, 2001). In
146 formulations for a hydrological model, the effect of the time scale of aggregation of the rainfall
147 data and the hydrological response of catchments of different sizes should be investigated in



148 order to identify the critical scale at which the resulting discharge will be the largest and could
149 potentially generate flash floods.

150 The most concentrating periods of precipitation are selected. Figure 7 shows the
151 instantaneous rainfall process from 6: 55 to 7: 35 on 7 June 2008. During this period, the
152 vapour concentrated on the southwest of Lantau Island, and transported northeast across the
153 mountains on Lantau Island. A large amount of precipitation was retained on the island.

154

155 **3.2 The 17-22 August 2005 storm**

156 August 2005 was much wetter than normal. A very active southwest monsoon during 17-22
157 August brought in plenty of moisture. Figure 3(d) shows contours of the total amount of
158 rainfall. The maximum total rainfall amount was 890 mm. The storm centre was at the middle
159 of the territory, Shatin. From Fig. 4, both the maximum rolling 4-h rainfall and 24-h rainfall of
160 the 17-22 August 2005 storm are least critical among the three storms investigated in this
161 paper. The storm caused 229 reported landslides, resulting in one fatality. The LPI value is 10
162 (Kong and Ng, 2006).

163 Figure 8 shows the instantaneous rainfall process from 10:35 to 11:15 on 20 August, 2005,
164 which is recognized as the heaviest rainfall period in this storm event. The prevailing moisture
165 inflow mainly came southerly during this period. The rainfall centre concentrated on the south
166 of Tai Mo Shan.

167

168 **3.3 The 21-24 July 1994 storm**

169 The total precipitation amount in the storm event from 21 to 24 July 1994 was recorded as the
170 highest for any consecutive days in July. The weather was related to a trough of low pressure
171 (Tam et al., 1995). Figure 3 shows contours of the total amount of rainfall of this storm
172 cantering at the middle of New Territories, Tai Mo Shan. The maximum total rainfall amount



173 was 1450 mm. In Fig. 4, the maximum rolling 24-h rainfall is the most critical, especially for a
174 smaller area. The storm caused 820 natural terrain landslides and 451 man-made slope failures,
175 resulting in 5 fatalities and 4 injuries. The LPI value is 10 (Chan, 1995).

176 Figure 9 shows the instantaneous rainfall process from 15:00 to 15:40 on 23 July 1994,
177 which records the heaviest rainfall process in this storm event. During this period, the moisture
178 air came from on the northwest of Tai Mo Shan. Most of precipitation concentrated on Tai Mo
179 Shan, and the spatial distribution of rainfall was quite uneven. As the moisture flux rose across
180 Tai Mo Shan, a large amount of moisture began to fall as rain. The orographic intensification
181 effect was very significant in this rainstorm event.

182

183 **3.4 Summary of the three large storms**

184 All the aforementioned three storms are related to monsoons other than typhoons. The
185 meteorological factors for these storms are beyond the scope of this paper. This research
186 focuses on the areal distribution of precipitation which is believed to be more relevant to the
187 evaluation of the performance of the slope safety system. Thus the maximum rolling rainfall
188 values are estimated in different durations. According to the records from the automatic rain
189 gauges, the maximum rolling rainfall among all the rain-gauge stations in each of the three
190 events can be calculated. The corresponding peak values and stations are summarized in Table
191 1. The 22-24 July 1994 storm is the largest among the three storms with regard to the amounts
192 of the maximum rolling 1-h and 24-h rainfall. However, in terms of the maximum rolling 4-h
193 rainfall, the 5-7 June 2008 storm is the most critical.

194 The contours of the total rainfall for the three storms, interpolated using a triangular
195 method, are shown in Fig. 5. The total precipitation amount of the 5-7 June 2008 storm is the
196 smallest among the three events, while that of the 21-24 July 1994 storm is the largest due to its
197 longer duration. However, the LPI value for the 5-7 June 2008 storm is 12, larger than those of



198 the other two storms; that is, the 5-7 June 2008 storm is the largest one in terms of damage. One
199 of the reasons is that the variability of spatial and temporal distributions of the storm affects
200 both the infiltration dynamics of the surface soil and the water levels above and below the
201 ground surface. The entire hydrological system is governed by the spatial and temporal
202 distribution of rainfall.

203

204 **4 Methodology of spatial analysis**

205 The varying space-time distribution of rainfall in Hong Kong is a result of the interaction
206 between governing meteorological covariates and local hilly terrain. Instead of attempting the
207 use of a physical model to capture the spatial characteristics, our analysis presents a two-step
208 approach in which a surface trend is firstly established to assess the spatial distribution of the
209 rainfall amount in a fixed duration, followed by a further analysis of the spatial correlation of
210 the detrended residuals.

211

212 **4.1 Determination of the expected precipitation trend surface**

213 A storm is a phenomenon with gradual geographical changes in space; the rainfall amount can
214 be simulated as a spatially correlated random field superimposed on a trend surface (Grimes
215 and Pardo-Igúzquiza, 2010). Such an artificial rainfall trend surface can be used to represent
216 design storms. One could comprehend that the rainfall is correlated with the local terrain and
217 the design storm centres are likely to be around the mountain peaks. Hong Kong has a
218 relatively small area, and an individual storm is usually designed to have one or two centres for
219 engineering design purposes (AECOM and Lin, 2015). Distinguishing two peaks is not
220 necessary as the distance between any two peaks will be small with regard to the scale of a
221 typical rainstorm.

222 Based on random field theory (Vanmarcke, 1977), the trend surface is the expected value



223 of the precipitation distributed over the rainfall domain, while the residuals are stationary and
224 not affected by any shift in the coordinate system. Thus the first step is to divide the spatial
225 distribution into a trend surface and residuals by finding a trend surface fitting function.
226 Though most natural processes like a storm exhibit spatial variability with complex trends, this
227 paper uses a polynomial function for simplicity. Denote observations of a storm as $z_i(x_i, y_i)$
228 ($i=1, 2, \dots, n$). The fitted values are $\hat{z}_i(x_i, y_i)$:

$$229 \quad z_i(x_i, y_i) = \hat{z}_i(x_i, y_i) + \varepsilon_i \quad (3)$$

230 where x and y define the location; and ε_i are residuals. The second-order polynomial trend
231 surface is:

$$232 \quad \hat{z}_i = a_0 + a_1x_i + a_2y_i + a_3x_i^2 + a_4x_iy_i + a_5y_i^2 \quad (4)$$

233 The coefficients, a_0, a_2, \dots, a_5 , are determined by minimizing the sum of the squares of the error
234 term using the ordinary least squares (OLS) analysis (Journal and Huijbergts, 1978):

$$235 \quad Q = \min \sum_{i=1}^n \varepsilon_i^2 = \min \sum_{i=1}^n [z_i(x_i, y_i) - \hat{z}_i(x_i, y_i)]^2 \quad (5)$$

236 The computed trend surfaces for the total rainfall amounts of the three storms and the
237 detrended residuals are shown in Fig. 10. The residuals of the rainfall amounts in different
238 durations are often assumed to be stationary. Taking the maximum 4-h rolling rainfall as an
239 example, the trend surface is

$$240 \quad \hat{z} = -45984 - 0.0337x + 0.1527y + (-1.5297x^2 + 3.4783xy - 2.7125y^2) \times 10^{-7} \quad (6)$$

241 The peak point on the surface is (77429, 77793); the maximum 4-h rainfall on the trend
242 surface is 425 mm. The maximum points (extreme values) on the trend surfaces of the three
243 storms are summarized in Table 3. The major and minor axes can be calculated as those of the
244 ellipse with rainfall value approaching zero. The directions and lengths of the trend surfaces are
245 summarized in Table 4. The major and minor axes of the trend surfaces are determined by least
246 squares fitting of the original rainfall data. For an individual storm event, the maximum points



247 of the trend surfaces are inside a relatively small range of 40 km. The storm centre of each
248 event on the trend surface agrees with the reality. The storm centres of the 7 June 2008 storm,
249 the 17-21 August 2005 storm and the 23 July 1994 storm are at west Lantau Island, Shatin and
250 Tai Mo Shan, respectively. The major directions of the spatial forms are between 19° and 43°
251 in the anticlockwise direction.

252

253 **4.2 Determination of the scale of fluctuation of precipitation residuals**

254 A classical way to characterizing the spatial correlation is through an autocorrelation function
255 (ACF), $\rho(h)$ (Fenton and Griffiths, 2008; Foresti and Seed, 2014). The autocorrelation
256 describes the correlation between values of a same series. The autocorrelation $r(k)$ for lags
257 $k=0, 1, \dots, m$, where m is the maximum number of lags, is evaluated by the following equation:

$$258 \quad r_k = \frac{\frac{1}{(N-k-1)} \sum_{i=1}^{N-k} (z_i - \bar{z})(z_{i+k} - \bar{z})}{\frac{1}{(N-1)} \sum_{i=1}^{N-k} (z_i - \bar{z})^2} \quad (7)$$

259 where z_i and z_{i+k} are the detrended storm depths at locations i and $i+k$, respectively; N is the
260 total number of the residuals; and \bar{z} is the mean value of the residuals.

261 In order to assess the autocorrelation structure of the detrended storm amounts, it is
262 necessary to perform regression analysis to fit the ACF. Among many correlation structures,
263 the single exponential structure is the most common:

$$264 \quad \rho(h) = \exp(-2h/\theta) \quad (8)$$

265 where h is the separation distance or lag; θ is the scale of fluctuation (SoF). The correlation ρ
266 (h) decays exponentially with separation distance h . The negative autocorrelation coefficient
267 will not be evaluated. The values of θ can be obtained accordingly. Within the scale of
268 fluctuation, the rainfall property is strongly correlated. A smaller scale of fluctuation indicates
269 more rapid fluctuations of the mean.



270 The scale of fluctuation is evaluated in the directions of N 0° E, N 45° E, N 90° E, and N
271 135° E for each storm. The values of SoF are fitted by an ellipse using least squares fitting. The
272 values of SoF and the fitting curves are shown in Figs. 11-13. Greater SoF values indicate
273 smaller variability. The major direction can be recognized as the direction of maximum
274 continuity.

275 The direction and major and minor scales of fluctuation are summarized in Table 4. The
276 SoF values of the rainfall residuals are between 6 to 37 km. Regardless of the variations of the
277 principal axis direction, the minor-axis lengths of the SoF values remain around 7 km (Table
278 4).

279

280 **5 Spatial description of rainstorms**

281 **5.1 Geometric spatial form and correlation structure**

282 Though rainfall varies over space, the rainfall amount of a particular storm in terms of
283 maximum rolling rainfall can be fitted by a polynomial function. The spatial form of the
284 rainfall amount can be represented by a rotated ellipsoid with only one centre. Such an artificial
285 spatial form may exhibit geometrical regularity. For each storm, the trend surfaces in different
286 durations show good consistency in the shape parameters in terms of the peak point, long-axis
287 direction and axis length. The peak points on the trend surfaces of the three storms are located
288 in a relatively small range. The long-axis directions of the spatial forms of each event in
289 different durations almost remain unchanged between 19° and 43°. The lengths of the major
290 and minor axes for an individual storm show consistency. The 5-7 June 2008 storm has the
291 largest impact area, as indicated by larger axis lengths among the three rainstorms according to
292 the results in Table 3.

293 With respect to the instantaneous rainfall processes shown in Figs. 7-9, the rainfall
294 distributions in terms of maximum rolling rainfall are quite consistent to the heaviest rainfall



295 process in each storm event. The rainfall distributions are strongly affected by the storm
296 humidity transportation, and are so uneven that the entire area should not be described as a
297 single site. The locations of the storm centres determine the general trend of the areal rainfall
298 distribution. The polynomial trend surfaces are effective for representing large rainstorm
299 distributions in terms of maximum rolling rainfall.

300 The spatial connectivity can be assessed by the SoF values. A smaller scale of fluctuation
301 indicates more rapid fluctuations of the mean. According to Figs. 11-13, all of the SoF values
302 are within 30 km, though the semi-lengths of the major axes of fitting curves are larger. Hence
303 a reasonable upper threshold for the spatial connectivity is estimated to be 30 km. On the other
304 hand, the lengths of the minor axis of the SoF values are between 5 to 8 km. The lower limit of
305 the SoF values of the rainfall data is considered to be 5 km. Therefore, the rainfall amount in
306 Hong Kong is observed to be strongly spatially correlated within 5 km, whose spatial
307 continuity is smaller than 30 km.

308

309 **5.2 Comparison with the spatial structures of ordinary rainfall events**

310 Besides the three large rainstorm events in this paper, ordinary rainstorm events in Hong Kong
311 have also been studied (Liu, 2013; AECOM and Lin, 2015). Liu (2013) proposed a framework
312 for analysing dynamic time-space evolution of rain-field in her thesis. Four rain events were
313 chosen to illustrate the spatial structure of rainfall in Hong Kong: the 18 May 2007, 19 May
314 2007, 19 April 2008 and 15 September 2009 rain events in Hong Kong. The 2008-04-19
315 rainstorm event was under a combined effect of Typhoon Neoguri and a northeast monsoon,
316 while the other three rainstorms were results of tropical depressions. The total rainfall amounts
317 during the four rainfall events on 18 May 2007, 19 May 2007, 19 April 2008 and 15 September
318 2009 were 67.0, 99.6, 157.9 and 130.3 mm, respectively. The spatial structures of the four rain
319 events indicated by variogram ranges corresponding to the peak rainfall intensity (six minutes



320 resolution) are plotted in Fig. 14. According to the results from ellipse fitting, the major
321 principal directions of all the tropical depression storms (i.e. on 18 May 2007, 19 May 2007,
322 and 15 September 2009) are around 45° . The lengths of the principal axis of the tropical
323 depression storms are within 30 km; while that of the 19 April 2008 storm is 40.8 km. The
324 correlation structures of the instantaneous rain processes are consistent with those of the three
325 large storms as illustrated in Section 5.1.

326 The spatial structure of annual maximum daily rainfall using the variogram model
327 provides additional information for generating design storms from another point of view.
328 According to the study conducted by Jiang and Tung (2014), the spatial variability represented
329 by a variogram is used to establish the rainfall depth-duration-frequency relationships. By
330 normalising the indicator semivariogram by the variance of the indicator data, the normalised
331 semivariances of the mean annual maximum daily rainfall and the maximum rolling 24 hour
332 rainfall of the three storms are shown in Fig. 15. Based on the samples and the fitted
333 exponential variogram model, the range of the mean of annual maximum daily rainfall is 7.1
334 km, which is close to the omnidirectional range values of the maximum rolling 24-hour rainfall
335 for the storms, particularly those for the 2008 storm and the 2005 storm. Thus, given a large
336 storm whose spatial distribution is relatively smooth, the range value will be close to that of the
337 annual maximum daily rainfall. The spatial structures of the three severe storms and the four
338 ordinary rainfall events do not differ significantly.

339 With aspect to the local terrain impacts, the major directions of both the three large
340 rainstorms and the ordinary rainfall events are all consistent with the mountain range alignment
341 in Hong Kong (Fig. 1). However the severe storms are highly uncertain and it is difficult to
342 ascertain and predict the future precipitation and extreme rainfall. Lu et al. (2013), Lu and Lall
343 (2016) and Najibi et al. (2017) suggest a potential direction to further study the associated
344 atmospheric circulation with moisture transport that has improved the predictability of extreme



345 rainfall and flood in various regions including western Europe, Midwest and Northeast of the
346 United States. The spatial structure found in this study also indicates that there might be a link
347 between the distribution and the convergence of the moist air into the Hong Kong region.

348

349 **6 Conclusions**

350 A random rain field model has been proposed to study the spatial characteristics of three large
351 landslide-triggering rainstorms in Hong Kong. The cumulative rainfall depths in terms of
352 maximum rolling rainfall in different durations are of particular importance for landslide
353 studies, and are taken as random variables in this study. Based on the study, the following
354 conclusions can be drawn:

355 (1) The amounts of maximum rolling rainfall in different durations share a dominating spatial
356 structure that can be represented by a rotated ellipsoid surface established using the
357 ordinary least squares method. The shapes change slightly in different durations for a
358 particular storm.

359 (2) The major principal directions of the surface trends of the three rain storms are between
360 19° (N 71° E) and 43° (N 47° E), and the principal major and minor axis lengths are
361 83-386 km and 55-79 km, respectively.

362 (3) The spatial connectivity of large storms in Hong Kong is estimated to be between 5 km
363 and 30 km. The rainfall amounts in the three large storms are observed to be strongly
364 correlated within 5 km and likely to be connected within 30 km.

365 (4) To verify the rationality and reliability of the spatial structures of large rainstorms, the
366 spatial characteristics of four ordinary rainfall events are also studied. The spatial
367 structures of the three large rainstorms are similar with those of the ordinary rainfall
368 events and consistent with the mountain range alignment in Hong Kong.

369



370 **Acknowledgements**

371 The authors would like to thank the Geotechnical Engineering Office (GEO) of the Civil
372 Engineering and Development Department (CEDD) for providing the rainfall data described in
373 this paper. This research is supported by the Research Grants Council of the Hong Kong SAR
374 (Nos. C6012-15G and 16202716).

375

376 **References**

377 AECOM and Lin, B.: 24-hour probable maximum precipitation updating study, GEO Report
378 No. 314, Hong Kong: Geotechnical Engineering Office, HKSAR, 2015.

379 Bacchi, B., and Kottegoda, N.: Identification and calibration of spatial correlation patterns of
380 rainfall, *Journal of Hydrology*, 165 (1-4), 311-348, 1995.

381 Barancourt, C., Creutin J.D., and Rivoirard, J.: A method for delineating and estimating rainfall
382 fields, *Water Resources Research*, 28, 1133-1144, 1992.

383 Berne, A., Delrieu, G., and Boudevillain, B.: Variability of the spatial structure of intense
384 Mediterranean precipitation, *Advances in Water Resources*, 32, 1031-1042, 2009.

385 Bouvier, C., Cisneros, L., Dominguez, R., Laborde, J. P., and Lebel, T.: Generating rainfall
386 fields using principal components (PC) decomposition of the covariance matrix: a case
387 study in Mexico City, *Journal of Hydrology*, 278(1), 107-120, 2003.

388 CEDD: Landslide Potential Index. Information Note 03/2009, Hong Kong: Geotechnical
389 Engineering Office, HKSAR, 2009.

390 CEDD: Management of Natural Terrain Landslide Risk, Information Note 03/2008; 5, Hong
391 Kong: Geotechnical Engineering Office, HKSAR, 2008.

392 Chan, W. L.: Hong Kong Rainfall and Landslides in 1994, GEO report No. 54. Hong Kong:
393 Geotechnical Engineering Office, HKSAR, 1995.

394 Chang, W. L., and Hui, T. W.: Probable Maximum Precipitation for Hong Kong, Reprint 482,



- 395 Hong Kong Observatory, Hong Kong: Hong Kong Observatory, HKSAR, 2001.
- 396 Dai, F. C., and Lee, C. F.: Frequency-volume relation and prediction of rainfall-induced
397 landslides, *Engineering Geology*, 59(3), 253-266, 2001.
- 398 Dasaka, S. M., and Zhang, L. M.: Spatial variability of in situ weathered soil, *Géotechnique*,
399 62(5), 375-384, 2012.
- 400 De Luca, D. L.: Analysis and modelling of rainfall fields at different resolutions in southern
401 Italy, *Hydrological Sciences Journal*, 59(8), 1536-1558, 2014.
- 402 Fenton, G. A., and Griffiths, D. V.: *Risk Assessment in Geotechnical Engineering*, John Wiley
403 & Sons, Inc., Hoboken, New Jersey, 2008.
- 404 Foresti, L., and Seed, A.: The effect of flow and orography on the spatial distribution of the
405 very short-term predictability of rainfall from composite radar images, *Hydrology and*
406 *Earth System Sciences*, 18, 4671-4686, 2014.
- 407 Gao, L., Zhang, L. M., and Chen, H. X.: Likely scenarios of natural terrain shallow slope
408 failures on Hong Kong Island under extreme storms, *Natural Hazards Review*,
409 10.1061/(ASCE)NH.1527-6996.0000207, B4015001, 2015.
- 410 Grimes, D. I. F., and Pardo-Igúzquiza, E.: Geostatistical analysis of rainfall geographical
411 analysis, *Geographical Analysis*, 42, 136-160, 2010.
- 412 Gyasi-Agyei, Y., and Pegram, G.: Interpolation of daily rainfall networks using simulated
413 radar fields for realistic hydrological modelling of spatial rain field ensembles, *Journal of*
414 *Hydrology*, 519, 777-791, 2014.
- 415 Jiang P., and Tung Y. K.: Incorporating daily rainfalls to derive rainfall DDF relationships at
416 ungauged sites in Hong Kong and quantifying their uncertainty, *Stochastic Environmental*
417 *Research and Risk Assessment*, 29(1), 45-62, 2014.
- 418 Journel, A. G., and Huijbergts, C. J.: *Mining Geostatistics*, London: Academic Press, 1978.
- 419 Kong, H. S. W., and Ng, A. F. H.: Factual report on Hong Kong rainfall and landslides in 2005,



- 420 GEO Report No. 223, Hong Kong: Geotechnical Engineering Office, HKSAR, 2006.
- 421 Lebel, T., Bastin, G., Obled, C., Creutin, J. D.: On the accuracy of areal rainfall estimation: a
422 case study, *Water Resources Research*, 23(11), 2123–2134, 1987.
- 423 Leung, J. K. Y., and Law, T. C.: Kriging analysis on Hong Kong rainfall data, *HKIE*
424 *Transactions*, 9 (1), 26-31, 2002.
- 425 Li, A. C. O., Lau, J. W. C., Cheung, L. L. K., and Lam, C. L. H.: Review of landslides in 2008,
426 GEO Report No. 274, Hong Kong: Geotechnical Engineering Office, HKSAR, 2009.
- 427 Li, X. Y., Zhang, L. M., and Li, J. H.: Using conditioned random field to characterize the
428 variability of geologic profiles, *Journal of Geotechnical and Geoenvironmental*
429 *Engineering*, 142(4), 04015096, 2015.
- 430 Liu, P.: Framework for analysing dynamic time-space evolution of rain-field, Mphil thesis,
431 The Hong Kong University of Science and Technology, 2013.
- 432 Lu, M., and Lall, U.: Tropical Moisture Exports, Extreme Precipitation and Floods in Northeast
433 US, *Hydrology and Earth System Sciences Discussions*, 0, 1-40, 2016.
- 434 Lu, M., Lall, U., Schwartz, A., and Kwon, H.: Precipitation predictability associated with
435 tropical moisture exports and circulation patterns for a major flood in France in 1995,
436 *Water Resources Research*, 49(10), 6381-6392, 2013.
- 437 Mascaro, G., Deidda, R., and Hellies, M.: On the nature of rainfall intermittency as revealed by
438 different metrics and sampling approaches, *Hydrology and Earth System Sciences*, 17,
439 355-369, 2013.
- 440 Panthou, G., Viscchel, T., Lebel, T., Quantin, G., and Molinié, G.: Characterising the space-time
441 structure of rainfall in the Sahel with a view to estimating IDAF curves, *Hydrology and*
442 *Earth System Sciences*, 18, 5093-5107, 2014.
- 443 Najibi, N., Devineni, N., and Lu, M.: Hydroclimate drivers and atmospheric teleconnections of
444 long duration floods: An application to large reservoirs in the Missouri River Basin,



- 445 Advances in Water Resources, 100, 153-167, 2017.
- 446 Rodríguez-Iturbe, I., Cox, D. R., and Eagleson, P. S.: Spatial modelling of total storm rainfall,
447 In Proceedings of the Royal Society of London A: Mathematical, Physical and Engineering
448 Sciences, the Royal Society, 403(1824), 27-50, 1986.
- 449 Tam, K. H. Au, C. H., and Chang, W. L.: The severe rainstorms on 22-24 July 1994 in Hong
450 Kong, Reprint 256, Hong Kong: Hong Kong Observatory, HKSAR, 1995.
- 451 Vanmarcke, E. H.: Probability modelling of soil profiles, Journal of the Geotechnical
452 Engineering Division, 103(11), 1227-1246, 1977.
- 453 World Meteorological Organization: Manual on Estimation of Probable Maximum
454 Precipitation (PMP), WMO-No.1045, Geneva, 2009.
- 455 Zawadzki, I. I.: Statistical properties of precipitation patterns, Journal of Applied Meteorology,
456 12(3), 459-472, 1973.



Table 1. Values of maximum rolling rainfall of three landslide-triggering storms in Hong Kong.

Duration	5-7 June 2008 storm		17-21 August 2005 storm		22-24 July 1994 storm	
	Amount (mm)	Station	Amount (mm)	Station	Amount (mm)	Station
1-hour	154	N21	82	N25	212	N14
4-hour	384	N19	174	N18	365	N14
24-hour	623	N19	570	N01	956	N14
2-day	672	N19	768	N01	1216	N14
4-day	768	N19	890	N01	1450	N14

Table 2. Locations of maximum rainfall on the trend surfaces (km).

Duration	5-7 June 2008 storm		17-21 August 2005 storm		22-24 July 1994 storm	
	Amount (mm)	Station	Amount (mm)	Station	Amount (mm)	Station
4-hour	(774, 778)		(822, 816)		(822, 836)	
12-hour	(764, 788)		(825, 822)		(822, 835)	
24-hour	(781, 752)		(829, 819)		(823, 833)	
36-hour	(769, 747)		(830, 820)		(825, 826)	



Table 3. Directions and lengths of the axes of trend surfaces.

Duration	5-7 June 2008 storm		17-21 August 2005 storm		22-24 July 1994 storm	
	Major axis direction (°)	Minor axis length (km)	Major axis direction (°)	Minor axis length (km)	Major axis direction (°)	Minor axis length (km)
4-hour	36°	229	42°	107	19°	72
12-hour	29°	253	40°	97	40°	62
24-hour	25°	269	38°	85	39°	77
36-hour	27°	386	35°	86	43°	79

Table 4. Directions and semi-lengths of the axes of scale of fluctuation (SoF).

Duration	5-7 June 2008 storm		17-21 August 2005 storm		22-24 July 1994 storm	
	Major axis direction (°)	Semi-lengths of the major axes (km)	Major axis direction (°)	Semi-lengths of the major axes (km)	Major axis direction (°)	Semi-lengths of the major axes (km)
4-hour	-18°	31	-3°	14	8°	7
12-hour	-7°	17	38°	37	21°	6
24-hour	-36°	12	33°	23	4°	6
36-hour	-79°	18	36°	24	9°	6

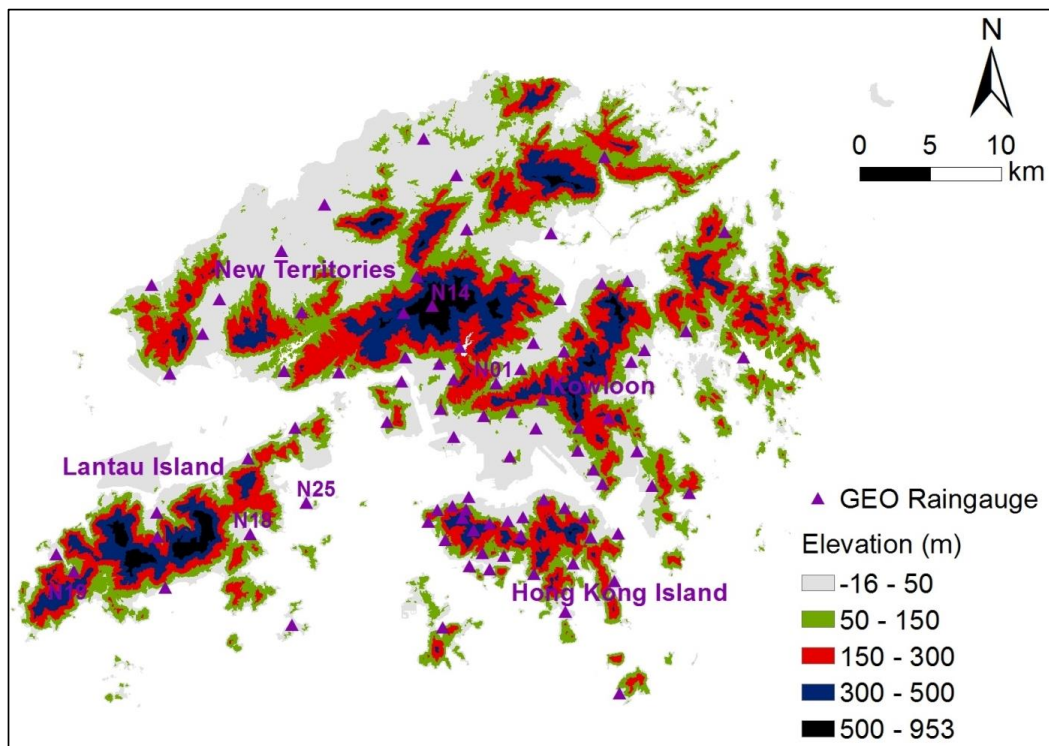


Figure 1. The GEO rain-gauge network in Hong Kong.

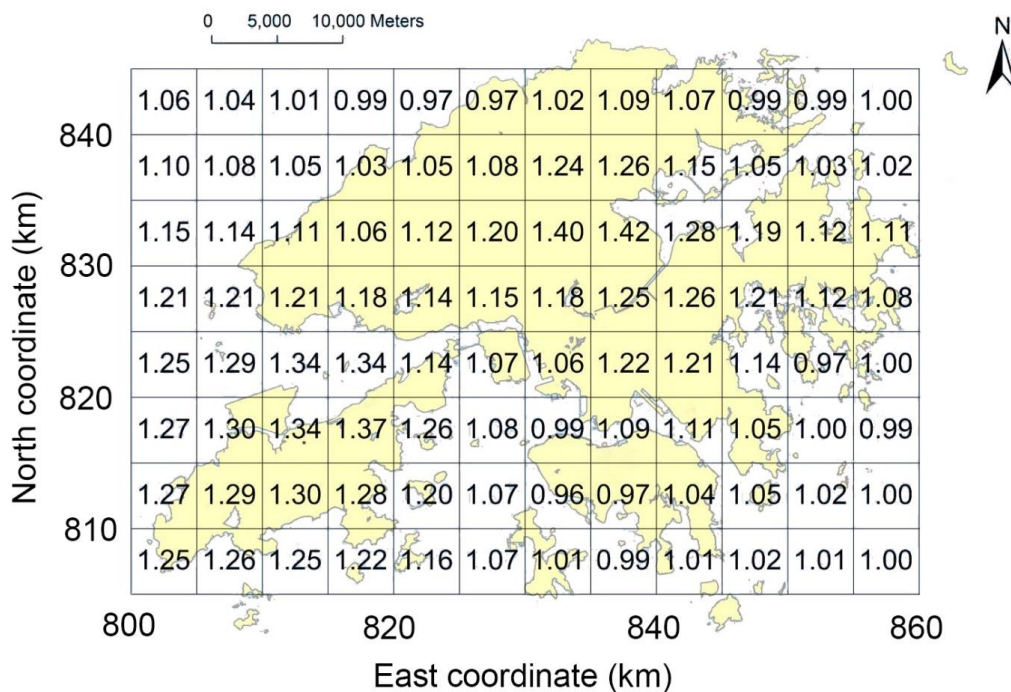


Figure 2. 24-hour orographic intensification factors in Hong Kong (modified from AECOM 2011).

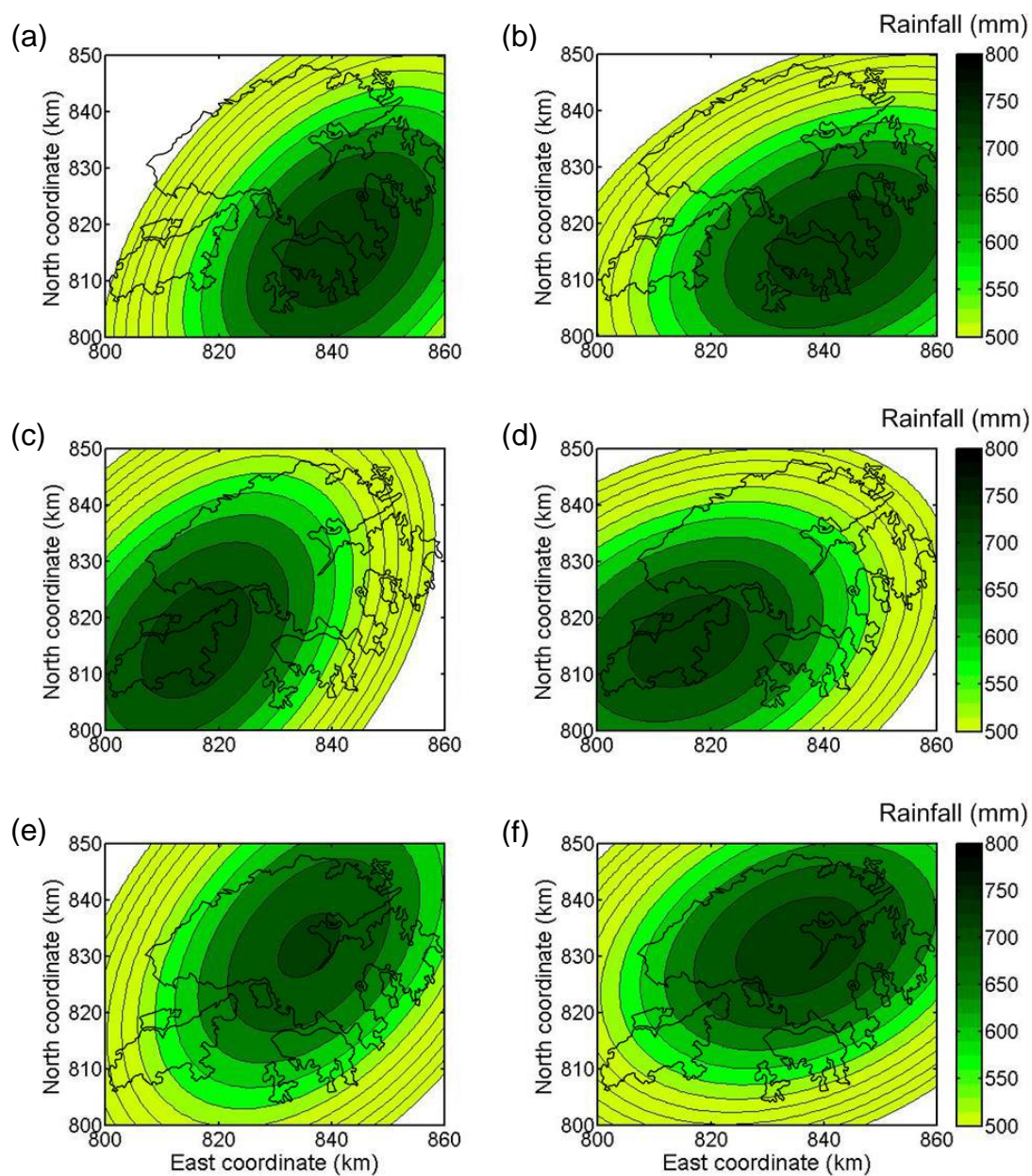


Figure 3. Generalized convergence component pattern with (a) NE-SW orientation 45° (b) ENE-WSW orientation 22.5° centred at Hong Kong Island; (c) NE-SW orientation 45° (d) ENE-WSW orientation 22.5° centred at Lantau Island; (e) NE-SW orientation 45° (f) ENE-WSW orientation 22.5° centred at Tai Mo Shan (modified from AECOM 2011).

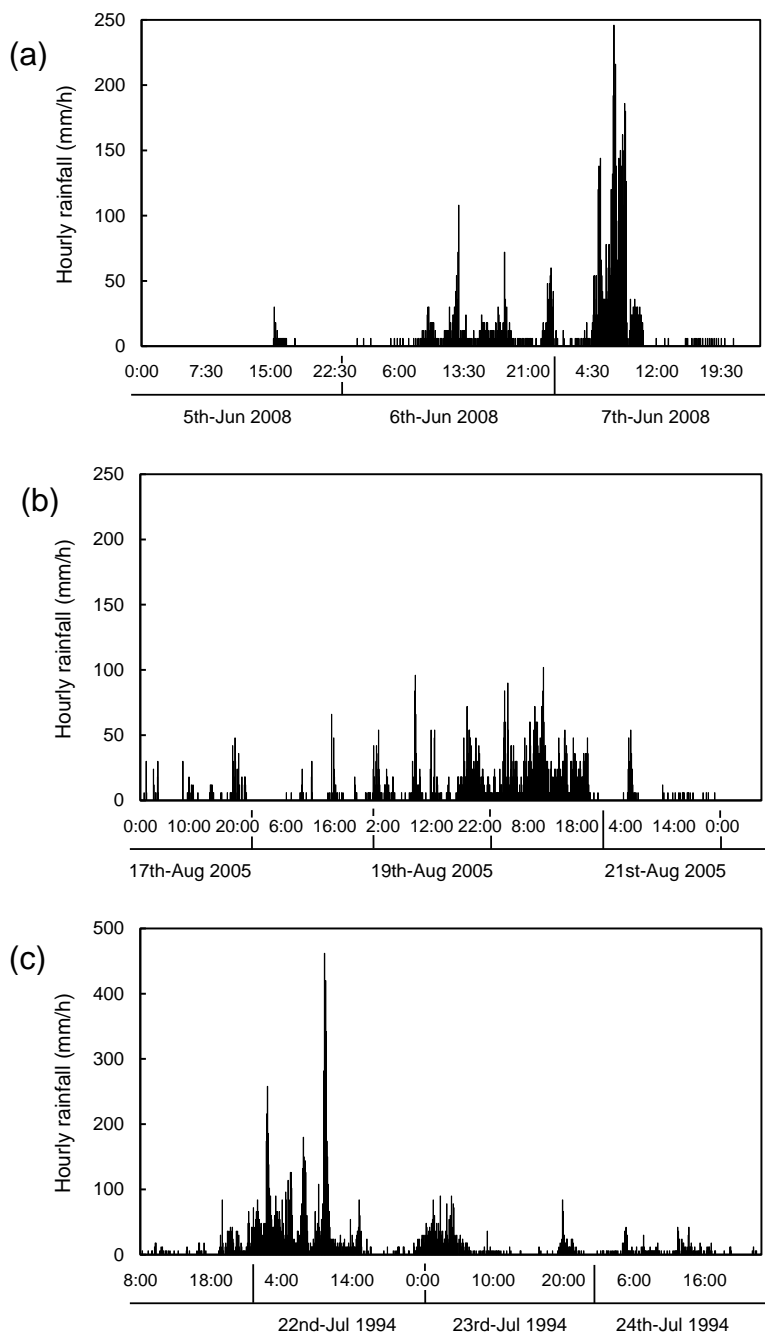


Figure 4. Hyetographs of three storms: (a) 5-7 June 2008 storm, Station N19; (b) 17-21 August 2005 storm, Station N01; (c) 22-24 July 1994 storm, Station N14.

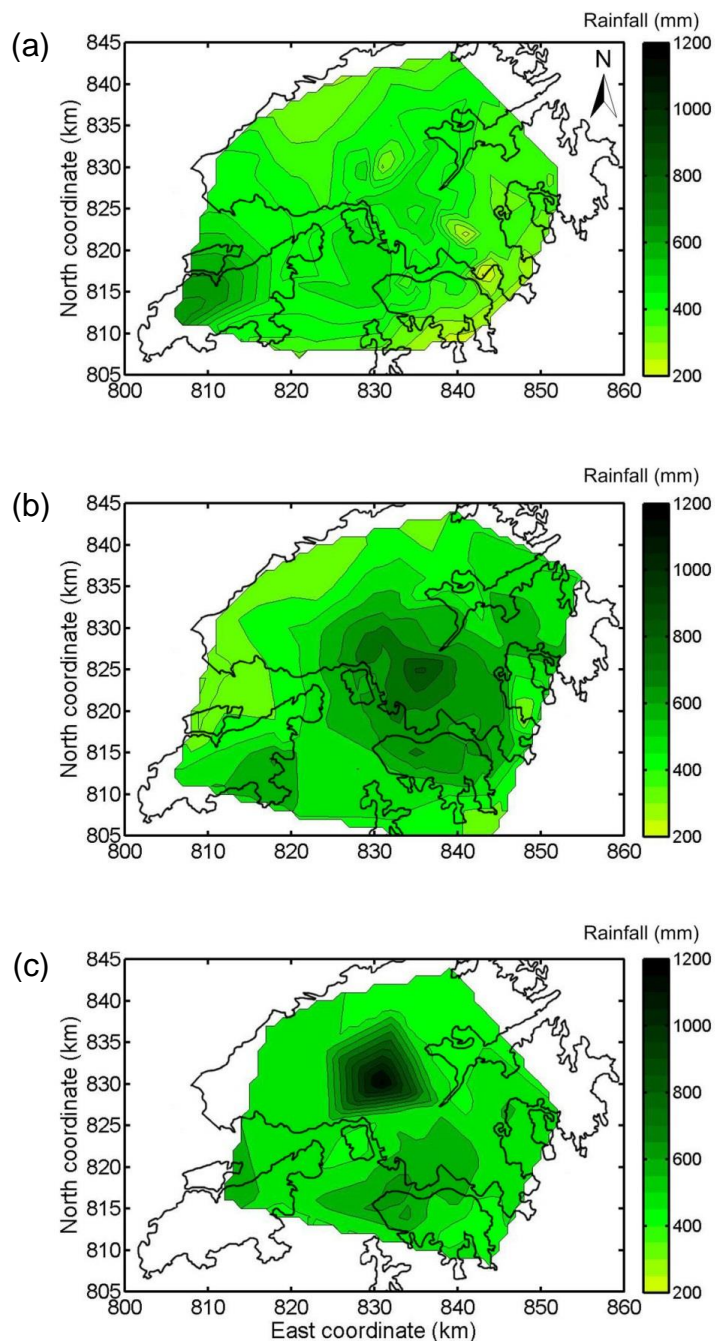


Figure 5. Spatial distribution of the total rainfall amount: (a) the 5-7 June 2008 storm; (b) the 17-21 August 2005 storm; (c) the 22-24 July 1994 storm.

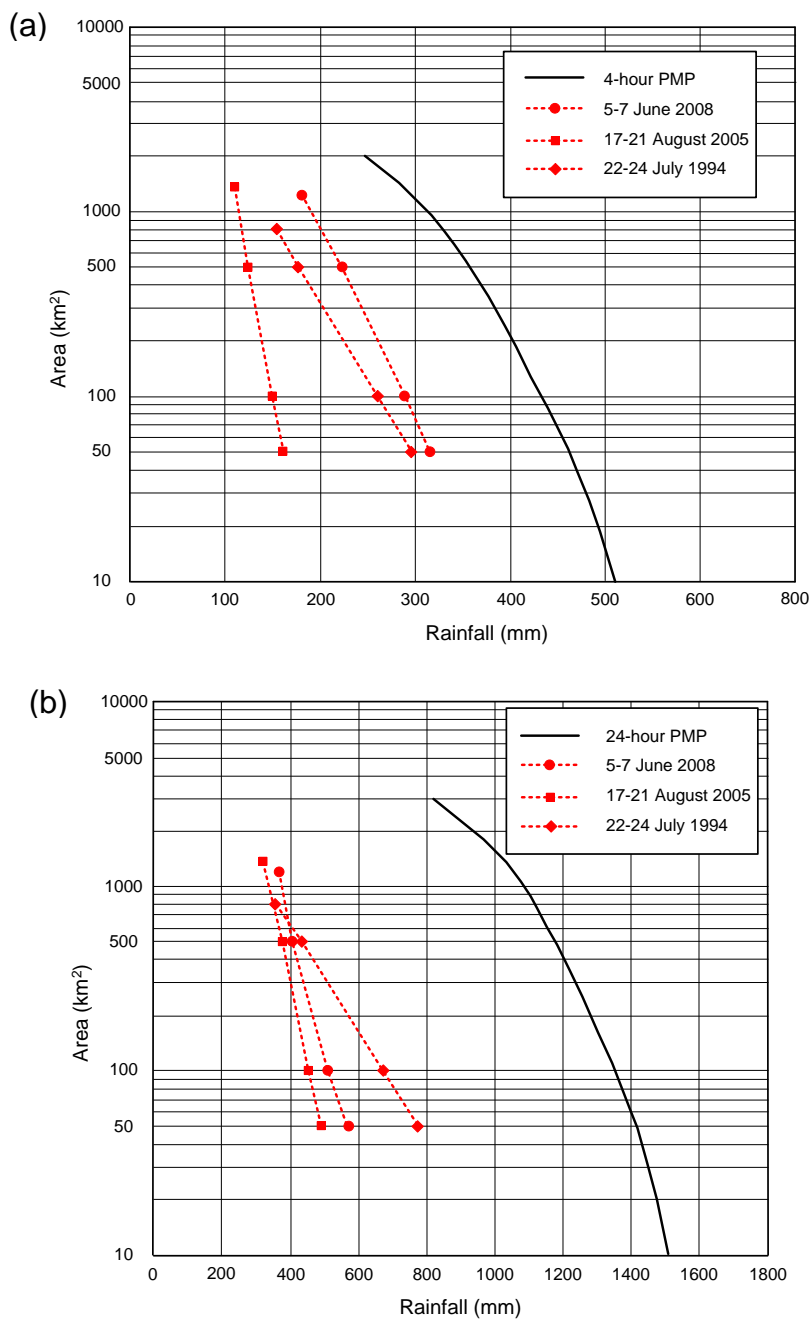


Figure 6. Magnitudes of the three storms characterized by (a) 4-h PMP, and (b) 24-h PMP (Modified from AECOM 2011).

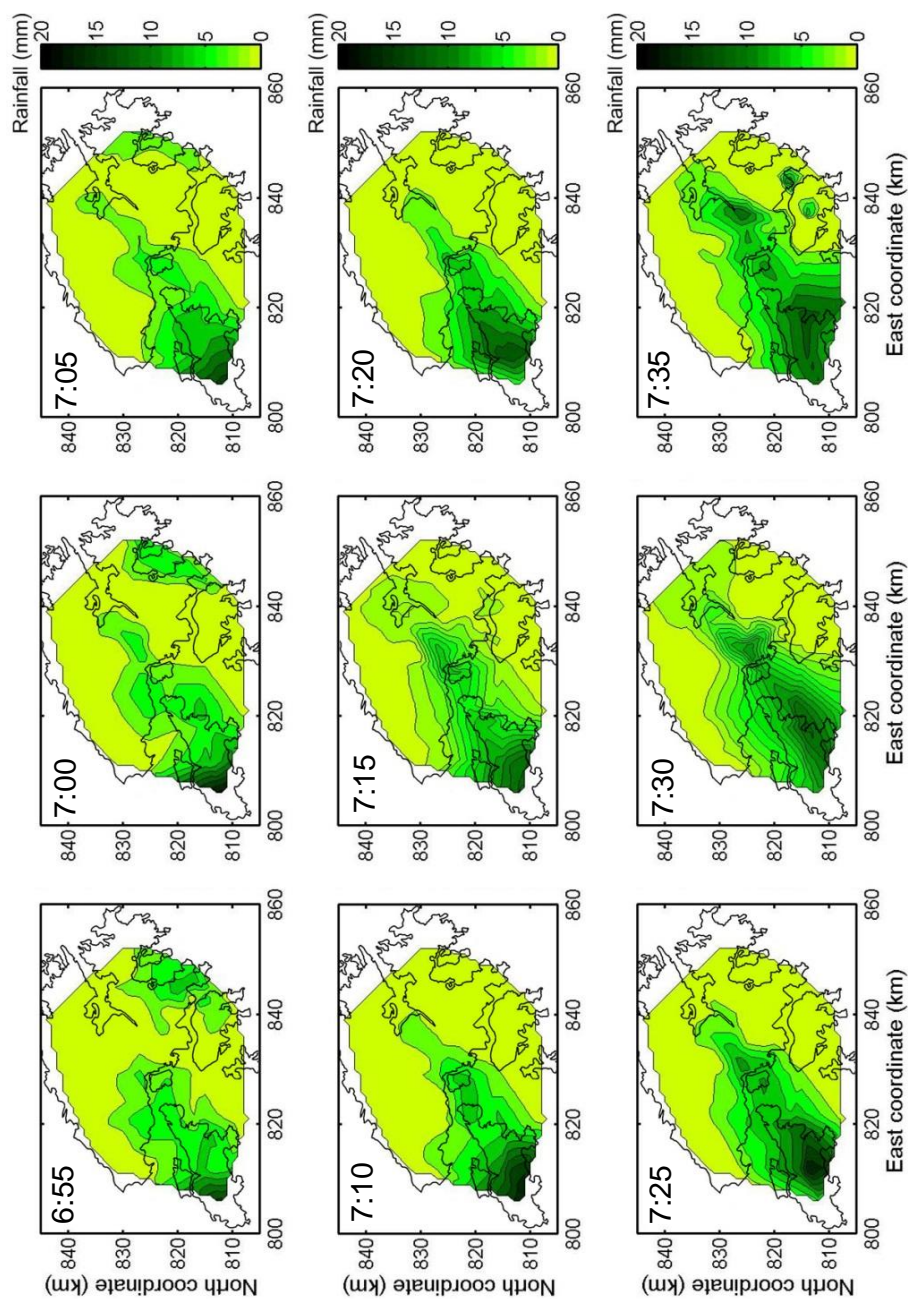


Figure 7. Instantaneous rainfall process from 6:55 to 7:35 on 7 June 2008.

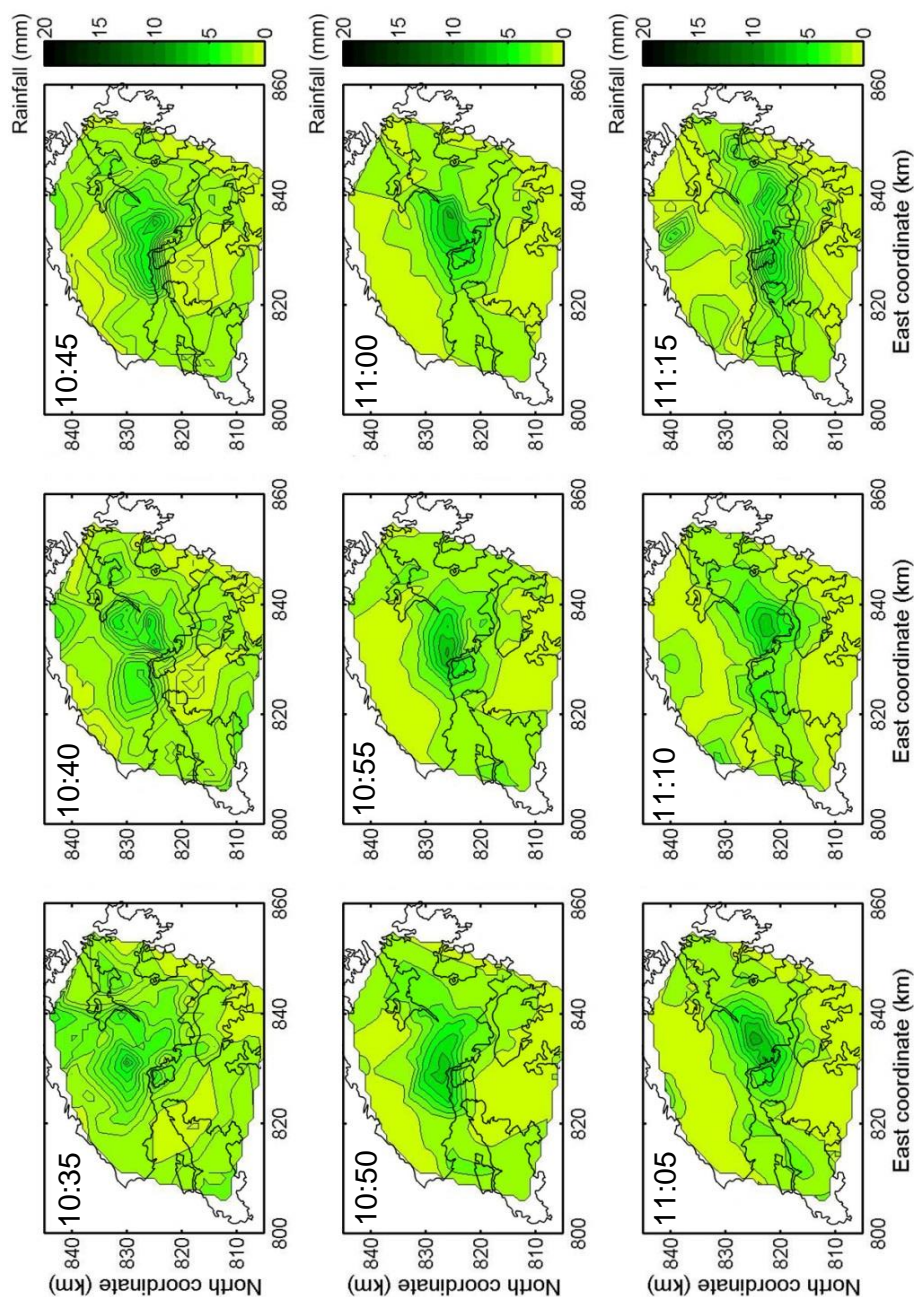


Figure 8. Instantaneous rainfall process from 10:35 to 11:15 on 20 August 2005.

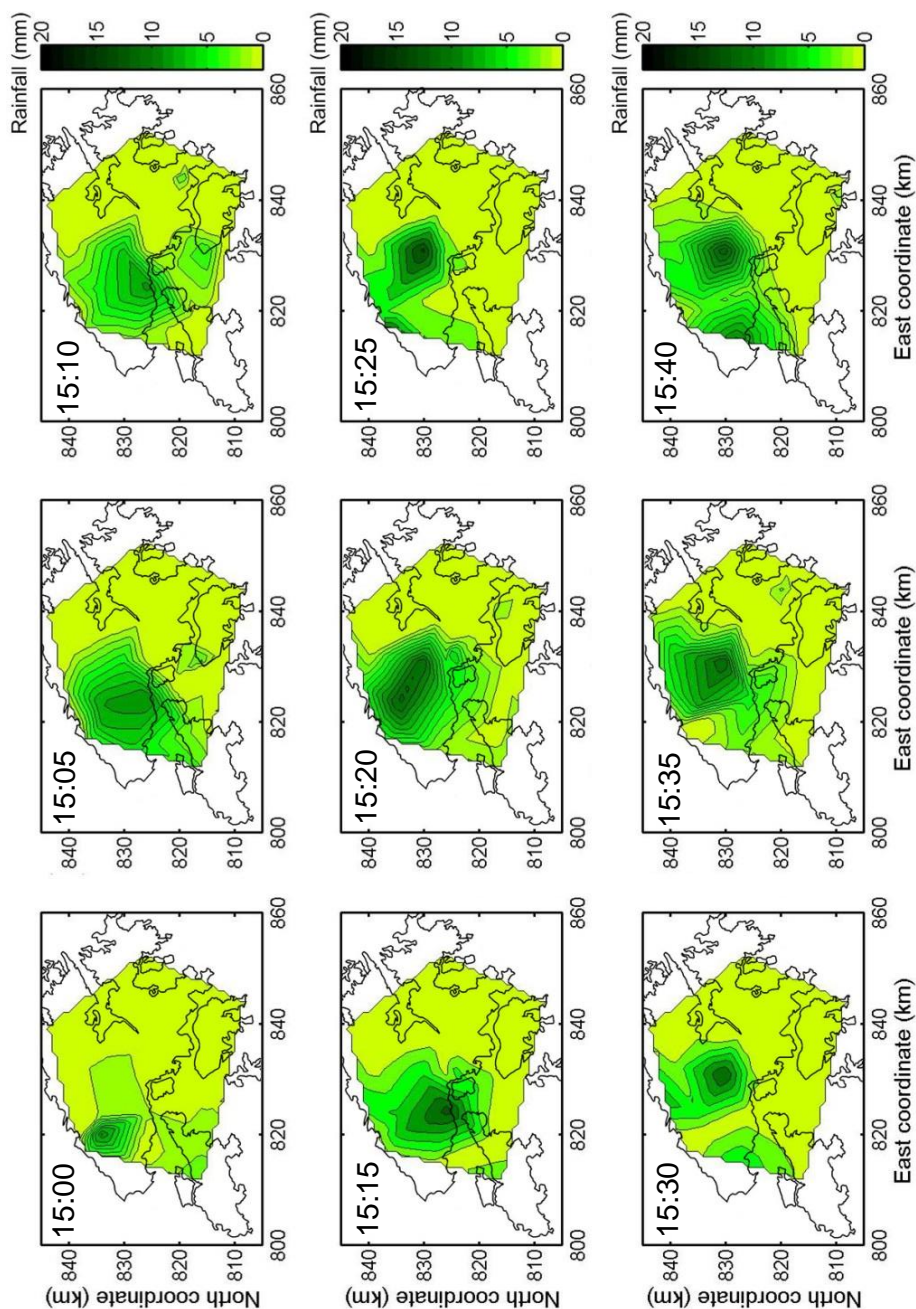


Figure 9. Instantaneous rainfall process from 15:00 to 15:40 on 23 July 1994.

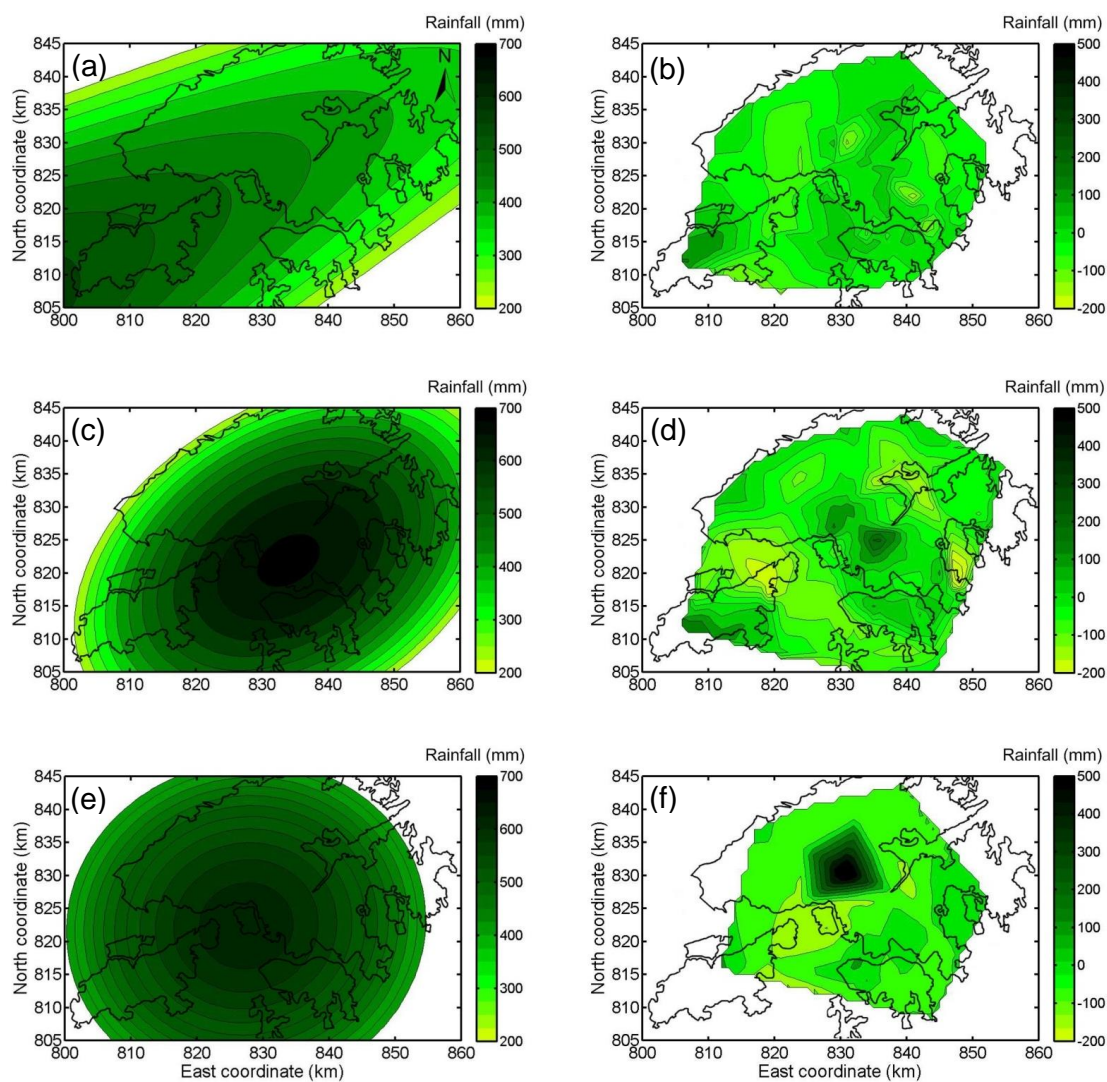


Figure 10. Trend surfaces and residuals of the total rainfall amounts: (a) and (b) the 5-7 June 2008 storm; (c) and (d) the 17-21 August 2005 storm; (e) and (f) the 22-24 July 1994 storm.

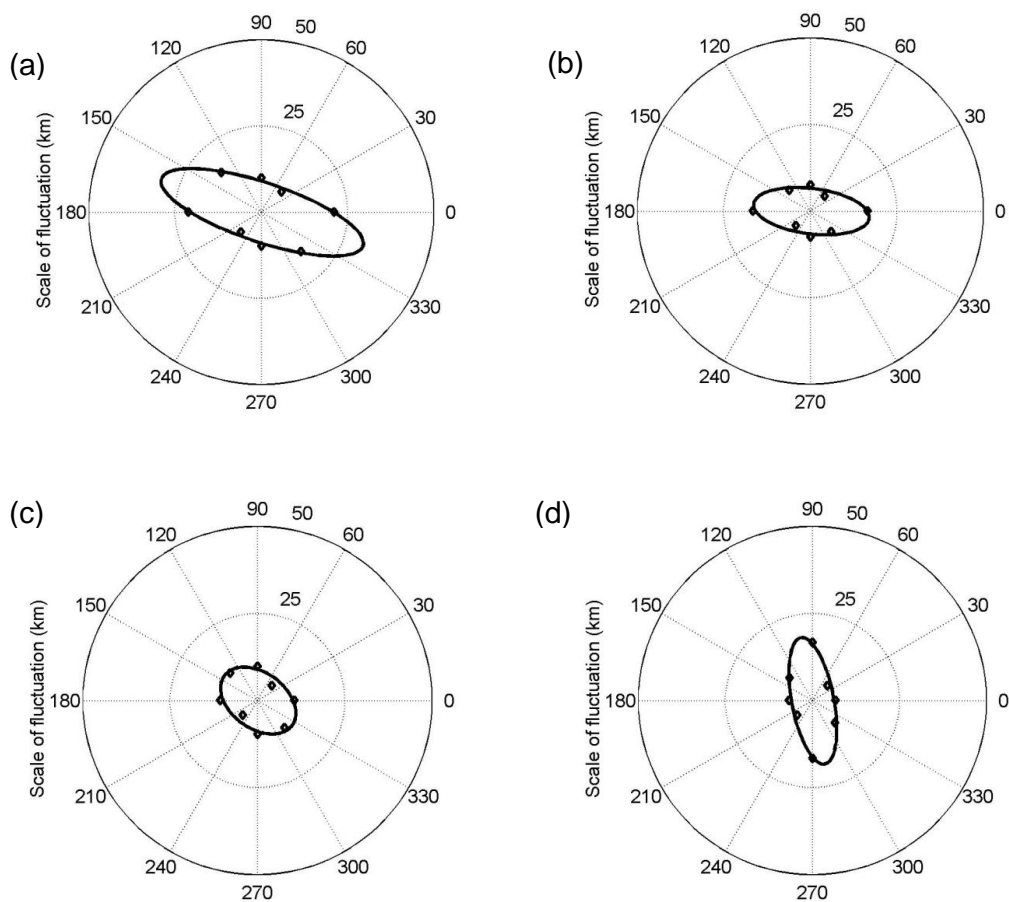


Figure 11. Scale of fluctuation values and ellipse-fitting curves for the 5-7 June 2008 storm: (a) maximum rolling 4-h rainfall, (b) maximum rolling 12-h rainfall; (c) maximum rolling 24-h rainfall; (d) maximum rolling 36-h rainfall.

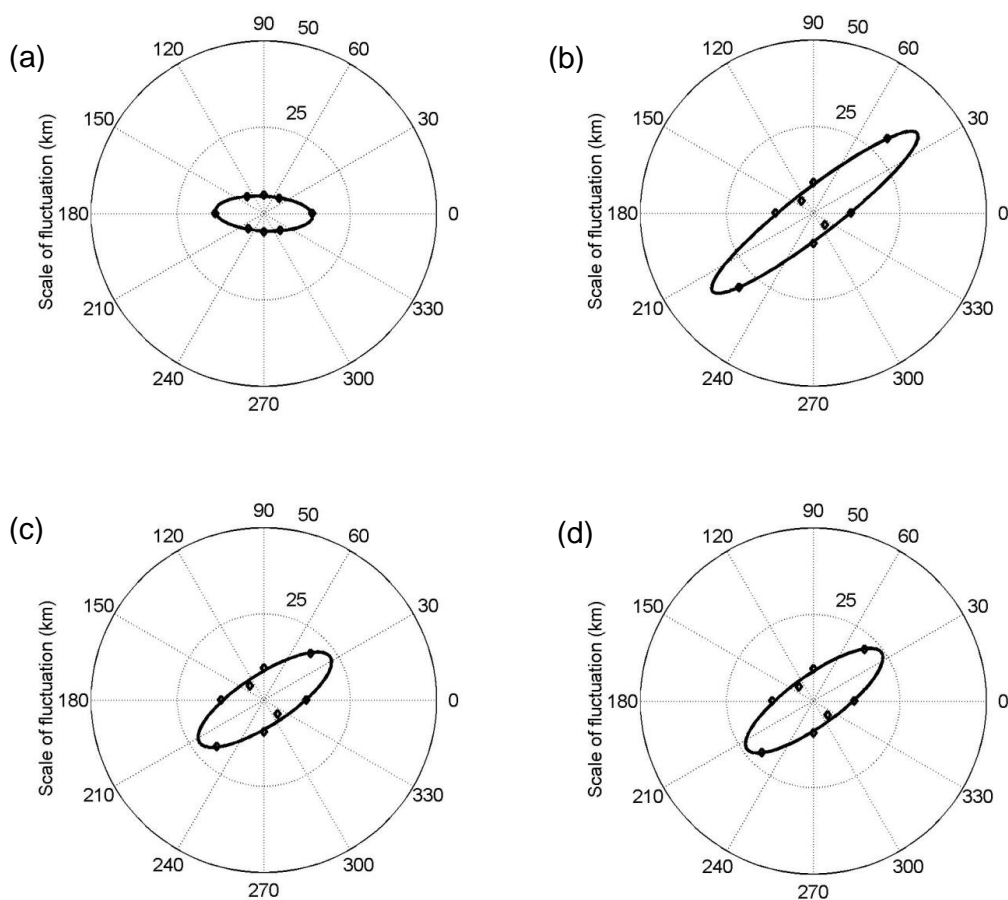


Figure 12. Scale of fluctuation values and ellipse-fitting curves for the 17-21 August 2005 storm: (a) maximum rolling 4-h rainfall; (b) maximum rolling 12-h rainfall; (c) maximum rolling 24-h rainfall; (d) maximum rolling 36-h rainfall.

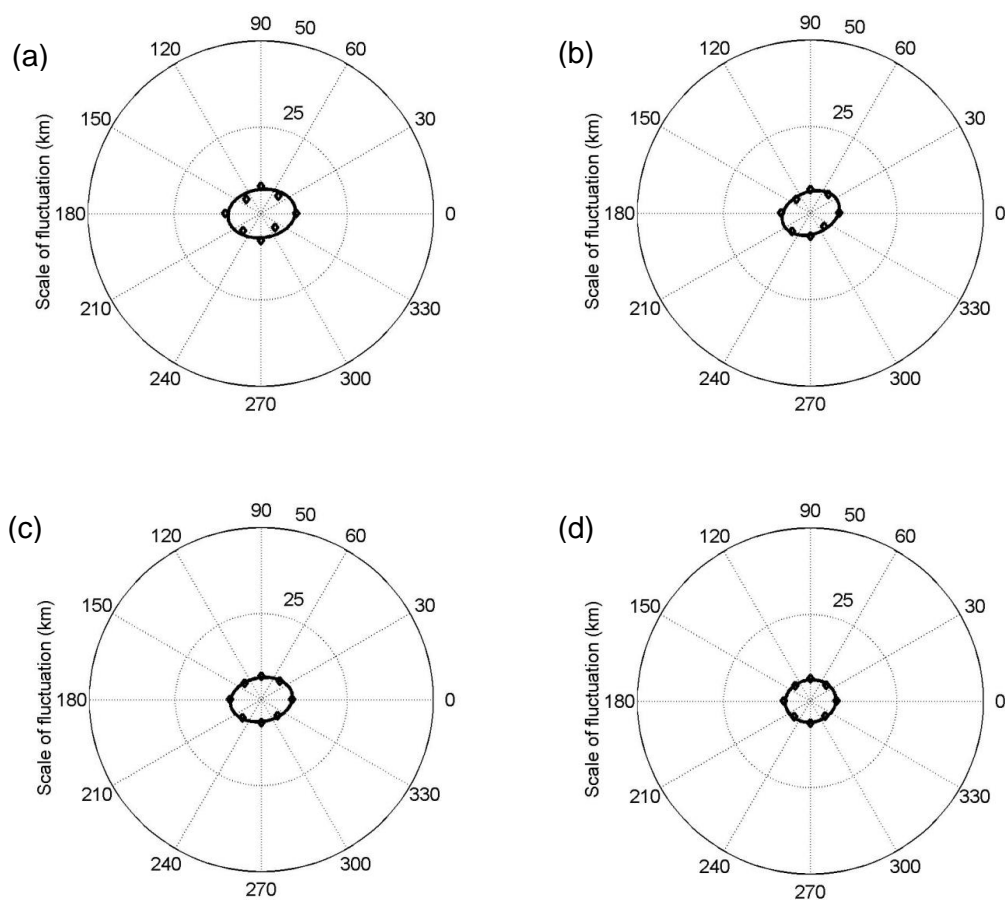


Figure 13. Scale of fluctuation values and ellipse-fitting curves for the 22-24 July 1994 storm:
(a) maximum rolling 4-h rainfall; (b) maximum rolling 12-h rainfall; (c) maximum rolling 24-h
rainfall; (d) maximum rolling 36-h rainfall.

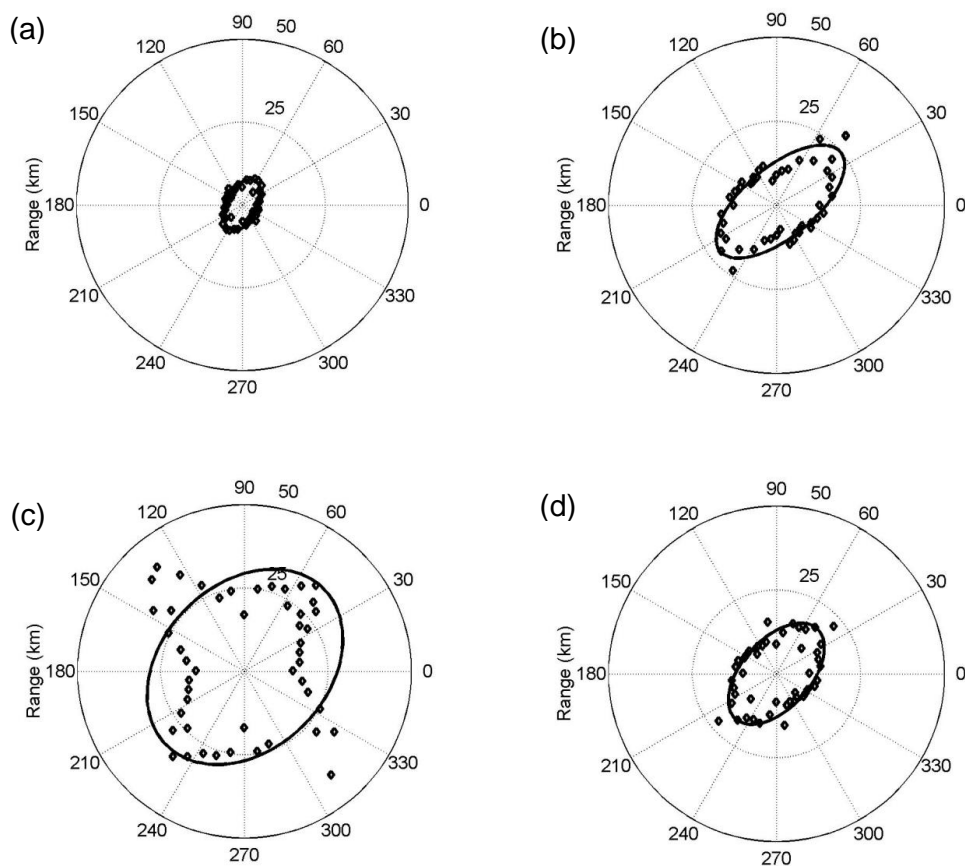


Figure 14. Range values for (a) the 18 May 2007 storm (16:30 pm); (b) the 19 May 2007 storm (16:00 pm); (c) the 19 April 2008 storm (20:00 pm); (d) the 15 September 2009 storm (15:00 pm) (modified from Liu 2013).

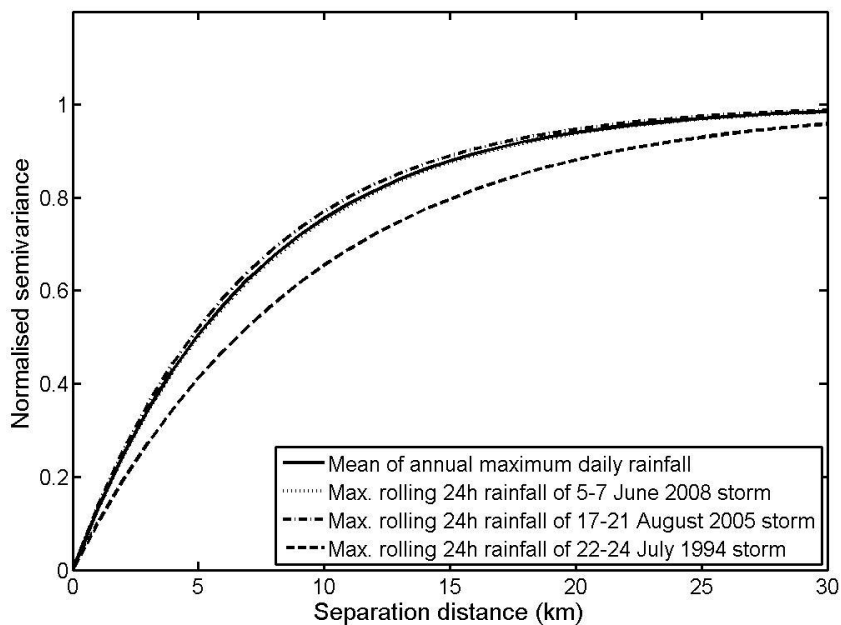


Figure 15. Normalised semivariances of the maximum rolling 24-hour rainfall of the three storms and the mean annual maximum daily rainfall in Hong Kong.